JS 24
ONDES AU SERVICE DES PLASMAS
PLASMAS AU SERVICE DES ONDES

Ray Tracing of Very Low Frequency Waves Produced by Active Experiments or Lightning Events at Low Earth Orbit

L. Cerfolli[1,2], J.-F. Ripoll[1,2], R. B. Horne[3], A. M. Wold[4], R. A. Marshall[4], G. W. Perry[5], A. D. Howarth[5], C. M. Cully[5]

[1] *CEA, DAM, DIF, F-91297, Arpajon, France*
[2] *UPS, CEA, LMCE, 91297 Bruyères-le-Châtel, France*
[3] *British Antarctic Survey, Natural Environment Research Council, Cambridge, England*
[4] *Department of Aerospace Engineering Sciences, University of Colorado, Boulder, CO, USA*
[5] *Department of Physics and Astronomy, University of Calgary, Calgary, Alberta, Canada*

Mots clés : Ray-tracing, Ondes très basses fréquences, Modèles de champs géomagnétiques, Basses orbites
Key words: Ray tracing, Very Low Frequency waves, Magnetic field models, Low Earth orbit

Summary

We investigate the propagation in the plasmasphere of Very Low Frequency (VLF) electromagnetic waves such as natural lightning-generated whistler waves and waves produced by active experiments. An active experiment is an artificial controlled disturbance of the low orbit space or the ionosphere. The aim is often to produce electromagnetic waves for removing high-energy particles (mostly electrons). We study the wave propagation parameters whether they are geometric, background, or intrinsic parameters, such as the magnetic field model, the ambient plasma density model of the plasmasphere, and the wave frequency. All of these parameters allow different behaviors of propagation which are discussed in this article.

Résumé

Nous explorons la propagation d'ondes électromagnétiques de très basses fréquences dans la plasmasphère telle que des ondes de type siffleur générées par les éclairs ou des ondes produites par des expériences actives. Une expérience active est une perturbation artificielle et contrôlée de l'espace proche Terre ou de l'ionosphere souvent dans l'idée de dépeupler cette région de particules de hautes énergies (le plus souvent des électrons).
Pour le faire, nous ordonnons les paramètres de propagation selon trois classes : les paramètres de fond, les paramètres géométriques et les paramètres intrinsèques. Les paramètres de fond regroupent le modèle de champ magnétique ainsi que celui de la densité plasmasphérique. Ils influent via leurs valeurs aux différents points de calcul ainsi que leurs gradients. Le paramètre intrinsèque ici établi est la fréquence de l'onde. Avec ces paramètres nous verrons que des comportements très différents sont accessibles.

The plasmasphere, named by Carpenter (1961), is the toroidal region of cold electrons (1-5 eV) located between the ionosphere from ~90 km of altitude up to ~1000 km (Blelly and Alcaydé, 2007) and its external limit, the plasmapause. The plasmapause is generally defined as the location where the electron density decreases by a factor 5 on a radial distance of ~ 3000 km (Carpenter and Anderson, 1992). The plasmapause generally locates at the 100 #/cc density level (Ripoll et al. 2022). Many types of electromagnetic waves propagate within the plasmasphere and we focus in this article only on very low frequency (VLF) waves as natural lightning-generated whistler (LGW) waves as well as waves produced by active experiments. An active experiment is an artificial controlled disturbance in the low orbit space or in the ionosphere. The aim is often to produce waves for removing high-energy particles (mostly electrons) which are source of hard radiations for orbiting satellites. As instances of active experiments, the most noticeable are Barium releases as CRRES-1991 (Schriver et Haerendel, 1991) and more recently the amplification of local waves by the rocket exhausts of hydrazine burn (Bernhardt et al. 2021). Here, we study the propagation of VLF waves through a parametric numerical study involving the HOTRAY code (Horne, 1989), varying various parameters such as the magnetic field model, the ambient plasma density model of the plasmasphere, and the wave frequency.
In the first part, we briefly describe the numerical code and method. The second part discusses the importance of the magnetic field model. The third part is dedicated to the description and role of the diffusive equilibrium model driving the electron density in the plasmasphere. The fourth section shows the influence of the wave frequency. Conclusions are gathered in the fifth section.

1 Simulation of wave propagation

We use the HOTRAY code (Horne, 1989) developed at the British Antarctic Survey (BAS) to simulate VLF waves. HOTRAY assumes that the ambient plasma is non relativistic, that waves amplitudes are small for applying both the linear theory and linear instabilities, and that the wavelengths are large compared with the scale size for variations of the ambient medium (i.e. the WKB approximation). Based on Eikonal approximation, the main resolved equations are given by:

$$\frac{d\overrightarrow{R}}{dt} = -\frac{\partial D/\partial \overrightarrow{k}}{\partial D/\partial \omega} = \overrightarrow{v}_g \qquad (1)$$

$$\frac{d\overrightarrow{k}}{dt} = \frac{\partial D/\partial \overrightarrow{R}}{\partial D/\partial \omega} \qquad (2)$$

Eq. 1 solves the propagation in space, where k is the position vector, t the time, D the dispersion term and k the complex wave vector. In HOTRAY, the choice is made to assume the pulsation ω is real in order to keep the frequency constant in time. In Eq. 1 the right hand side can be identified as the wave group velocity. Eq. 2 solves for the evolution of the wave vector according to the dispersion relation.
In all point along the ray path, we have to solve the full dispersion relation

$$D(\overrightarrow{R}, \overrightarrow{k}, \omega) = 0 \qquad (3)$$

The complete expression of the dispersion relation is given in (Horne, 1989) and Eq. 3 can be written as
$An^4 + Bn^2 + C = 0$.
Furthermore, the numerator in the right hand side of Eq. 2 can be developed as

$$\frac{\partial D}{\partial \overrightarrow{R}} = \frac{\partial D}{\partial \overrightarrow{B}}\frac{\partial \overrightarrow{B}}{\partial \overrightarrow{R}} + \frac{\partial D}{\partial N}\frac{\partial N}{\partial \overrightarrow{R}} + \frac{\partial D}{\partial \overrightarrow{k}}\frac{\partial \overrightarrow{k}}{\partial \overrightarrow{R}} \qquad (4)$$

The three terms in the right hand side of Eq. 4 highlight the competition between magnetic field gradients, density gradients, and variations of the wave vector. In the third term, dk/dR, the variations in position of the wave vector account for changes in amplitude and geometry of the wave vector.

The fact that the wave vector is complex implies the wave amplitude can be damped or amplified. The wave vector direction is defined by two angles: the wave normal angle defined as the angle between the wave vector and the local magnetic field and the azimuthal angle defined as the geographic eastward component of the wave vector.
Background parameters regrouping the magnetic field and the density model appear as gradients in Eq. (4) as well as single point values in the dispersion relation.

An important condition for wave propagation is dictated by the lower hybrid (LH) frequency. The LH frequency is the limit for allowing the bounce of the ray at high latitude (see more below). Its definition is given by:

(5)

$$\omega_{LH} = [(\Omega_i\Omega_e)^{-1} + \omega_{pi}^{-2}]^{-1/2}$$

where $\Omega_i = \frac{q_i B}{m_i}$, is cyclotron pulsation, q_i is the charge, m_i is the mass, e and i indices refer to electrons and ions respectively, and ω_p is plasma pulsation. The lower hybrid frequency is proportional to the local magnetic amplitude, through the cyclotron pulsation term, and to the square of the electron density. An increase in B or in $\sqrt{n_e}$ increases the lower hybrid frequency. This shows another competition between the magnetic field and the plasma density for each single location of the wave during its propagation.

2 Influence of the magnetic field model

Active experiments are generally performed at low Earth orbit (from 100 km to 1500 km) and produce electromagnetic waves in a large range of L-shells according to the experiment altitude and latitude. The L-shell is the Earth's radius normalized distance of a given field line at the magnetic equator. The L-shell discriminates the field lines and depends on the chosen magnetic field model. At low Earth orbit (LEO), there are three main models for Earth's magnetic field: the pure dipole used by many codes for simplicity, as HOTRAY, the eccentric tilted dipole which is the most accurate dipolar approach of the Earth's magnetic field, and the full International Geomagnetic Reference Field (IGRF) model. Dipolar models have orthogonal metrics in classic space coordinates (as geographic or magnetic coordinates) which provides mathematical simplifications. The eccentric tilted dipole is a pure dipole for which the main axis is not the Earth's rotation axis, since it is tilted, and the magnetic center is not corresponding to the geographic center, since it is shifted. The IGRF is defined by a potential as a harmonic development around a tilted dipole field and is based on a potential defined from ground measurements. The potential expression is:

$$V(r,\theta,\varphi,t) = R_e \sum_{n=1}^{N} R^{n+1}[g_n^m \cos(m\varphi) + h_n^m \sin(m\varphi)]P_n^m(\cos(\theta)) \qquad (6)$$

where coefficients noted h and g are established from ground measurements, R_e is the Earth's radius, $R = R_e/r$, r is the radial distance, θ is the latitude, φ is the longitude and P_n^m are associated Legendre polynomials.
The magnetic field is then derived from the potential as

$$\vec{B} = -\vec{\nabla}(V) \qquad (7)$$

We use the 13th generation of the IGRF coefficients (Alken, 2020).

In Figure 1, we plot the magnetic amplitude with respect to latitude and longitude at 100 km of altitude. This altitude is chosen since it is the commonly adopted limit for electron precipitations in the upper atmosphere. Both the eccentric tilted dipole model and the IGRF model have the same main structures. First, the 'S shape' is the global shape along longitude produced by the variation of the magnetic equator along longitude. The second is the South Atlantic Anomaly (SAA), which is a zone of large depression in magnetic amplitude. The center of this depression is different between the eccentric tilted dipole and the IGRF models. For the eccentric tilted dipole, the center is at -30° of latitude and -10° of longitude while, for IGRF, it is centered at -40° of latitude and between -60° and -30° of longitude. This depression is a consequence of both the tilted axis and the shift of the magnetic center. The global shape of the SAA is also different for the two models. In the IGRF model, high order harmonics (n>3 in Eq. 5) constrain the SAA to fit with ground measurements.

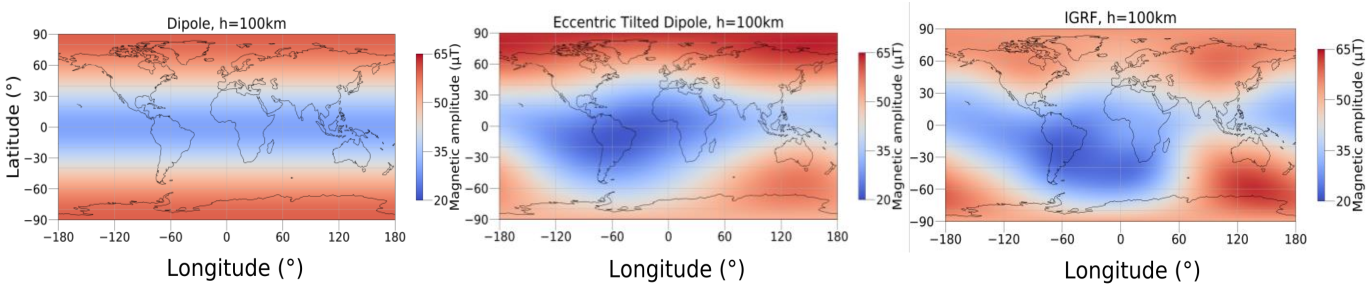

Figure 1: Mapping of the magnetic field amplitude at 100 km from (left) a pure dipole as used in HOTRAY, (center) the eccentric tilted dipole, and (right) the IGRF 13th generation model.

In Figure 2, we plot the relative error between the two dipolar models and the IGRF. Differences for each comparison are located around the IGRF SAA. The relative error reaches a maximum of 101% for the dipole and 53% for the eccentric tilted dipole. Elsewhere, dipolar models are rather accurate. However, the relative error does not show topologic differences seen on the field lines (not discussed here). Field lines end up different for each model, with implication on the propagation as field lines act as a wave guide. Note that, for very low frequency waves, the plasmapause also acts a wave guide (Inan et Bell, 1977). The consequence is that ray paths can change.

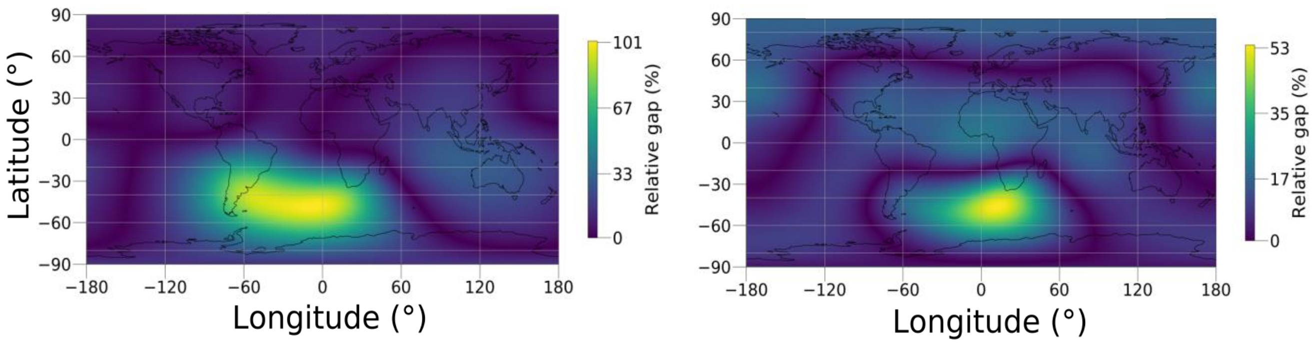

Figure 2: Mapping of the amplitude relative error at 100 km, (left) for a pure dipole field compared with IGRF and (right) from eccentric tilted dipole compared with IGRF. Most of the error is concentrated in the SAA region.

3 Influence of the plasmaspheric density model

The HOTRAY code computes ray-path evolving in an ambient medium filled of cold ions and electrons. Their density is given by the diffusive equilibrium model, which equates the electron density with the ionic densities $N_e = N_i$. The diffusive equilibrium further decompose N_i in:

$$N_i = N_b N_{de} N_{li} N_{pl} \qquad (8)$$

where N_b is the density on a given point at an altitude R_b. N_b is a scale density which scales the density profile in the whole plasmasphere. N_{de} is the profile of diffusive equilibrium along the radial direction, which depends on temperature T_{DE}, and gravity, $g(R_b)$, for each plasma component, as follows

$$N_{de}(R)^2 = \sum_{i=1}^{n} \eta_i \exp(-G/H_i)$$
$$H_i = \frac{k_B T_{DE}}{M_i m_p g(R_b)} \qquad (9)$$

In equations (9), in the profile of the diffuse equilibrium, each exponential is weighted by the proportion of the plasma component ions, η_i, which is a function of the radial distance. There are three available species: H+, He+, O+. This highlights the importance of the characteristic length of thermal diffusion, H_i, for each component of the ambient plasma. The associated thermal velocity is given by $v_{th} \approx \sqrt{(3k_B T_{DE}/m)}$. G is the geopotential height, k_B is the Boltzmann constant, M_i is the mass number for the ion labeled i, and m_p the proton mass.

N_{li} is a decreasing exponential function defined from the chosen altitude of the bottom ionosphere R_0, up to its height H (Eq. 10).

$$N_{li} = 1 - \exp[-(R - R_0)^2/H^2] \qquad (10)$$

N_{pl} introduces a latitude dependence through the L-shell value and curves the density isolines with the plasmapause shape, at position L_p expressed in L-shell.

$$N_{pl} = e^{-\frac{(L-L_p)^2}{H_p^2}} + (1 - e^{-\frac{(L-L_p)^2}{H_p^2}})(\left(\frac{R_c}{R}\right)^a + (1 - \left(\frac{R_c}{R}\right)^a)(e^{-(R-R_c)^2/H_s^2} \qquad (11)$$

H_p is the half width of the plasmapause boundary in L value. R_c is the geocentric distance in km to the level at which the density outside the plasmapause field line is equal to the density inside. H_s is the scale height of radial density decrease. And a determines how the density falls off outside.

The following subsections are dedicated to the influence of the diffusive equilibrium temperature, directly influencing the diffusion of the electron density, the absolute value of the electron density, and, finally, the wave frequency in HOTRAY simulations of VLF waves.

3.1 Influence of the diffusive equilibrium temperature

For each component, the characteristic length of thermal diffusion is proportional to the ratio of temperature with gravity so that, for a given position, as gravity is fixed, the scale length becomes directly proportional to temperature. In Figure 5, we vary the diffusive equilibrium temperature from T=1000 to 2000 K and show the variation of the electron density. Note that the scale density is fixed at $n_e = 2.7\ 10^9\ \#.m^{-3}$ (see section 3.2). The temperature radially diffuses density at higher radial distance and follows the fixed plasmapause at $L_p = 4.5$ (for all simulations). The diffusive scale length increases with temperature so that, as the temperature increases, more plasma components can reach higher altitudes driven by their thermal velocity.

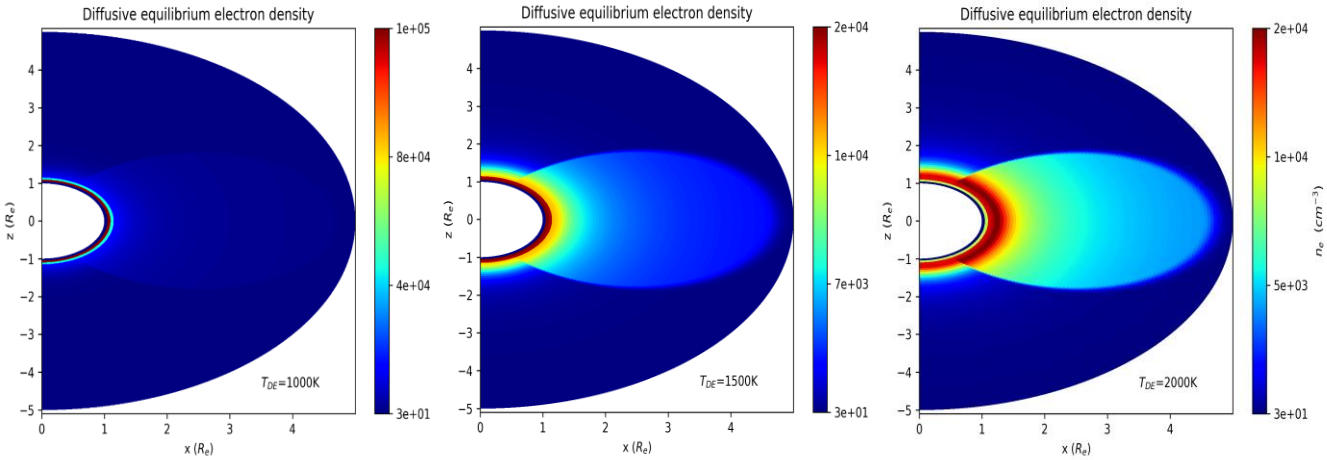

Figure 5: variation of the diffusive equilibrium electron density with temperature, (left) at 1000 K, (center) at 1500 K, (right) at 2000 K.

We present in Figure 6 four rays launched at -40° of latitude and 400 km of altitude into a plasmasphere computed using the diffusive equilibrium at temperature varying from 1000 to 4000 K. For all rays, we find the ray path is the same, except that it is shorten as the temperature increases. This is due to the shape of density isolines, which remains the same but the value of the isodensity is different according to the temperature. The more the density values is large, the more matter the wave passes through. This causes the waves to be more affected by Landau damping as the temperature increases, thus waves vanish earlier on the path.

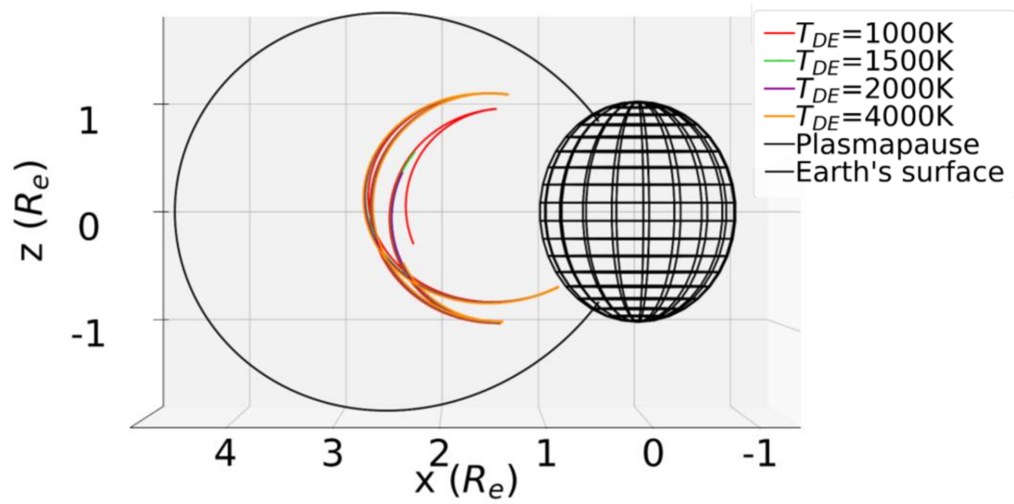

Figure 6: Ray paths of a 5 kHz ray for different temperatures, from T=1000 to 4000 K. The ray path is the same but shortens as the temperature increases.

3.2 Influence of the density scaling

In Eq. (7) the density parameter, N_b, scales all values of density in the plasmasphere leading to different behaviors for a given wave. In Figure 7, we propagate a 5 kHz wave for different values of Nb. For low density, the magnetic field dominates the propagation allowing the wave to reach the atmosphere on the conjugate point of the launch location and to vanish without bouncing (e.g. red line in Fig. 7). The magnetic field acts as a wave guide for the propagation. At high latitude, when density is high enough compared with the magnetic field, the lower hybrid frequency can exceed the wave frequency and permits the lower hybrid resonance to occur. In that case, the wave resonance cone is reduced to zero as the surface of refractive index becomes closed. A normal propagation (i.e. perpendicular propagation) to the local magnetic field is thus allowed so that the wave normal angle can reach 90°. As the wave propagates perpendicularly, its wave normal angle will exceed 90°, so that the wave is reflected back. A bounce has happen. Several of these magnetic bounces can occur in a common propagation. This effect is combined with the previous effect (density effect). More the encountered density is high, more the wave damping is strong and so the ray path is shortened along the ray path.

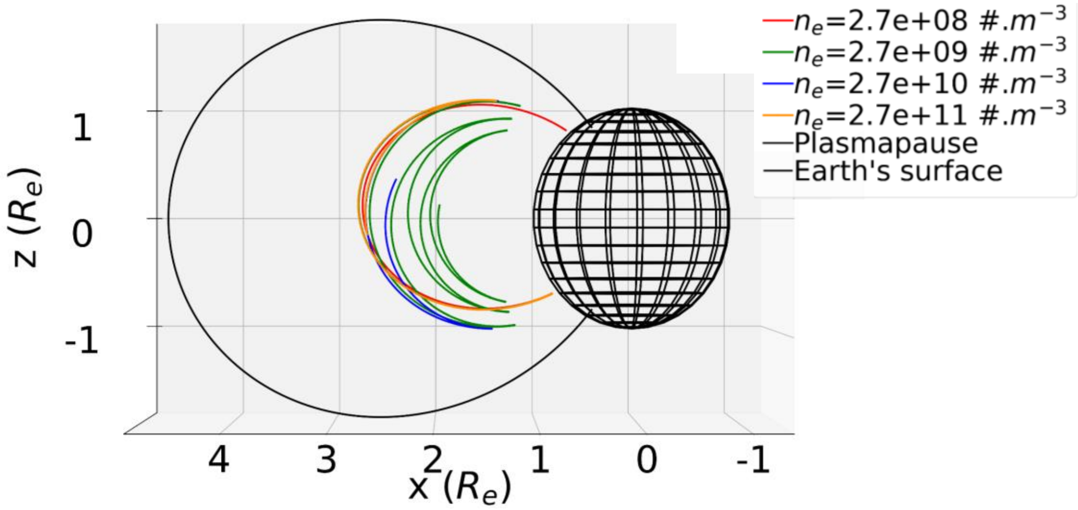

Figure 7: Ray paths of a 5 kHz wave for different scale density at 2000 K. With higher density at fixed magnetic amplitude magnetoreflections are allowed.

4 Influence of wave parameters: the frequency

Here, we study the importance of the frequency as this parameter influences the escape point from the ionosphere, the bounce at high latitude, and the region reached by the wave. Using a temperature of 2000 K and $n_e = 2.7\ 10^9\ \#.m^{-3}$, we propagate several waves at frequencies ranging from 1 kHz to 15 kHz within the plasmasphere. The 15 kHz ray only follows the field line because the lower hybrid frequency never comes near the wave frequency so that magnetoreflections are never allowed and the ray continues to follow the field line. This ray reaches the Earth's surface before its wave normal angle can reach the 90° critical value for allowing propagation in the opposite direction. Lower frequency rays (from 1 to 10 kHz) are now able to bounce between the two hemispheres. The lowest frequency waves at 1 and 2 kHz have bounced trajectories which are outward directed (each mirror points have increasing altitude). However, higher frequency waves (5 and 10 kHz) have an inward propagation after the first bounce, i.e. the following mirror points altitude is decreasing. This is due to a competition between the magnetic field shape and the density.

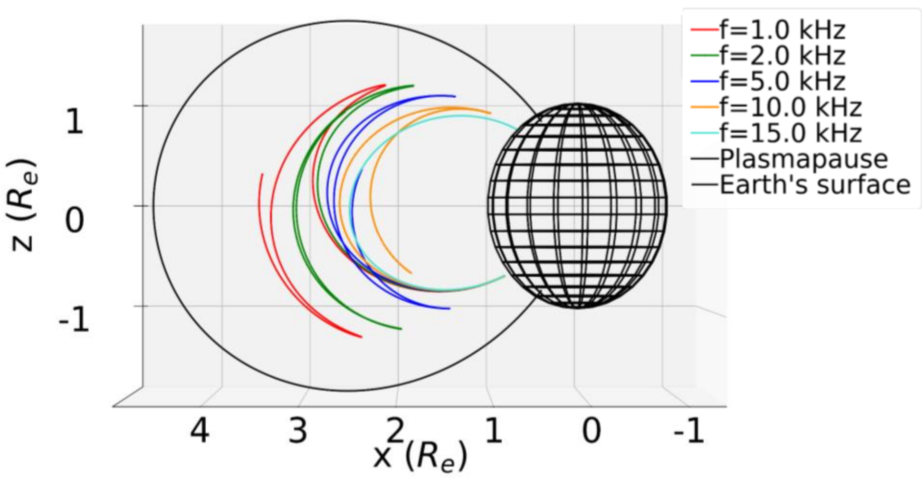

Figure 8: Ray path for several frequencies at 2000 K. The 15 kHz wave does not bounce since the lower hybrid frequency is never reached. Inward and outward propagation is allowed according to the frequency values from 1 kHz to 10 kHz.

5 Conclusions

In this article, we study the main parameters of the propagation of very low frequency waves in the plasmasphere using the BAS HOTRAY code. Comparing various magnetic field models we find that the relative error betwenn a pure dipole model and the IGRF model reaches a maximum of 96% in the SAA region. The relative error reduces to 53% for the eccentric tilted dipole. An ongoing task is to implement the IGRF model into HOTRAY. The density model has two main parameters, the temperature of the diffusive equilibrium and the scale density, which we study. The temperature diffuses the density to higher L-shells. We find it does not change the ray path but shorten them as temperature increases due to stronger Landau damping. The scale density defines isodensity curves which can allow (or not) magnetoreflections according to the value of the lower hybrid frequency. Finally, the frequency determines whether or not the propagating wave bounces. As the bounce is allowed, the propagation remains outward for low frequency waves. For higher frequencies, the propagation evolves to an Earthward propagation once the first bounce has occurred.

References

Carpenter, D. L., and R. R. Anderson (1992), An ISEE/whistler model of equatorial electron density in the magnetosphere, *J. Geophys. Res.*, 97(A2), 1097-1108, doi:10.1029/91JA01548.

P.-L. Blelly, D. Alcaydé: Ionosphere, in: Y. Kamide, A. Chian, Handbook of the Solar-Terrestrial Environment, Springer-Verlag Berlin Heidelberg, pp. 189–220, 2007. doi:10.1007/113677588

Ripoll, J.-F., Thaller, S. A., Hartley, D. P., Cunningham, G. S., Pierrard, V., Kurth, W. S., et al. (2022). Statistics and empirical models of the plasmasphere boundaries from the Van Allen Probes for radiation belt physics. Geophysical Research Letters, 49, e2022GL101402. https://doi.org/10.1029/2022GL101402

Horne, R. B., (1989), Path-integrated growth of electrostatic waves: the generation of Terrestrial Myriametric Radiation, J. Geophys. Res., 94, 8895-8909.

Schriver, D., and G. Haerendel (1991), Stimulated auroral precipitation by wave-particle interactions: Implications for the CRRES satellite mission, J. Geophys. Res., 96(A7), 11403–11419, doi:10.1029/91JA00668.

Alken P, Chulliat A, Nair M (2020) NOAA/NCEI and University of Colorado candidate models for IGRF-13. Earth Planets Space. https://doi.org/10.1186/s40623-020-01313-z

Inan, U. S., and T. F. Bell, (1977), The plasmapause as a VLF wave guide, J. Geophys. Res., 19, 2819.